Development of Series Elastic Actuators for Impedance Control of an Active Ankle Foot Orthosis

Bruno Jardim, jardim@sc.usp.br
University of São Paulo at São Carlos, Mechanical Engineering Department, Mechatronics Laboratory, Av. Trabalhador São-carlense, 400 - São Carlos,SP, Brazil

Adriano A. G. Siqueira, siqueira@sc.usp.br
University of São Paulo at São Carlos, Mechanical Engineering Department, Mechatronics Laboratory

Abstract. *This paper deals with force and impedance control of series elastic actuators for driving the joints of an exoskeleton for lower limbs. Series elastic actuators are devices where elastic components are introduced between the motor's output and the load. From the deflection of these components, it is possible to measure the force applied to the load and to control it. Also, the mechanical impedance of the actuator/load interface can be regulated to the typical values of joint's stiffness and damping presented by humans during the walking. Results of force and impedance control applied to an active ankle-foot orthosis driven by a series elastic actuator are presented. Also, a variable impedance control strategy is performed to reproduce the behavior of an actual ankle joint.*

Keywords: *Active orthoses, exoskeleton, force control, impedance control*

1. Introduction

The interface between an actuator and its load is commonly designed to be as rigid as possible, (Pratt & Williamson 1995). Increasing stiffness improves precision, stability and position control bandwidth. However, the use of such interface may incur some problems like: friction, torque oscillations and noise. According to (Pratt & Pratt 1998), an impedance control interface is generally required when there is human-machine contact. In these cases, unexpected contacts and external disturbances may be avoided to not harm the user.

Examples of devices where human-machine interaction is present are exoskeleton and active orthoses. Exoskeletons are being developed around the world to help physically weak or injured people and to increase the power of soldiers. The BLEEX (Berkeley Lower Extremity Exoskeleton), project support by the Defense Advanced Research Projects Agency (DARPA), uses hydraulic actuators supplied by a pump connected into a small gasoline engine (Kazerooni 2005, Zoss, Kazerooni & Chu 2005, Chu, Kazerooni & Zoss 2005). More than 40 sensors together with the actuators form a local net that works as the human nervous system (Kim, Anwar & Kazerooni 2004). The sensors constantly give information to the central computer that calculates the necessary action to distribute the weight in such a way that the soldier does not feel the exceeding weight. In (Walsh, Paluska, Pasch, Grand, Valiente & Herr 2006), an underactuated and lightweight exoskeleton that considers the passive dynamic of walking, differently of the one described above, is being developed. Two architectures are explored: the first one considers a spring in the hip, a variable impedance device in the knee and a spring in the ankle; the second one substitutes the spring of the hip for a no conservative actuator to examine the effect of power addition during the walking cycle. In this paper, it is considered the design and construction of the ankle joint of an exoskeleton, that is, the construction of an active ankle-foot orthosis.

Series elastic actuators are considered in this work since they present ideal characteristics for use in human-machine interaction: force control, impedance control (possibility of low impedance), impact absorption, low friction and bandwidth (Robinson, Pratt, Paluska & Pratt 1999, Sensinger & Weir 2006). The idea behind the series elastic actuator is the inclusion of an elastic component between the motor's output and the load. The measurement of the elastic deformation is related to the applied load force, trough the dynamic characteristic of the spring. In (Pratt, Krupp & Morse 2004), series elastic actuators are used in the development of a device for power augmentation of the knee joint. The same actuator is used in (B. & Herr 2004) to drive an active ankle-foot orthosis specially designed to deal with the drop foot pathology. In this paper, the series elastic actuator proposed in (Pratt & Williamson 1995) is reproduced to be used as driver of the proposed ankle-foot orthosis. Experimental results of force and impedance control are presented. Also, a variable impedance control strategy is performed to reproduce the typical values of ankle joint's stiffness and damping presented by humans during the walking.

This paper is organized as follows: Section 2.presents the active ankle-foot orthois design; Section 3.describes the series elastic actuator, its dynamic model, and the force and impedance control designs; Section **??** presents the results of the force and impedance controls applied to the active ankle-foot orthosis and the variable impedance control strategy.

2. Active Ankle-Foot Orthosis

In this section, the design and construction of the active ankle-foot orthosis is described in details. Actually, this device is the first constructed component of the exoskeleton for lower limbs based on a commercial orthosis being developed by the authors. The commercial orthosis corresponds to one reciprocating gait orthosis LSU (Lousiana State University). Figure 1 shows the orthosis and the first exoskeleton design.

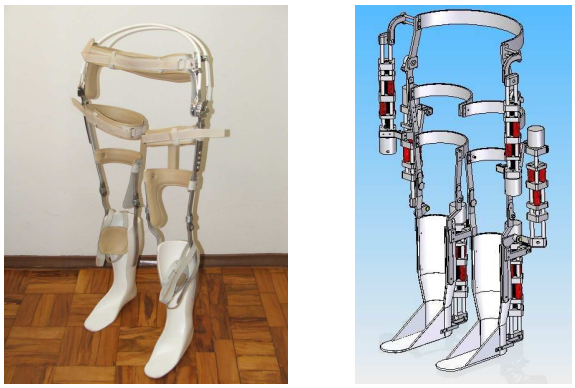

Figure 1. Commercial orthosis and exoskeleton design.

For the active ankle-foot orthosis design, anthropometric measures - such as limb dimensions and masses - normally observed in a healthy human were considered. Also, the ankle joint ranges of a normal gait pattern are used as input to the actuation mechanism design. To meet the bio-mechanical and structural needs of the project, and to provide a fixation point to the series elastic actuator and to the sensors, the following mechanical design was conceived, Figure 2. The series elastic actuator is mounted on the back of the device and moves the ankle-foot orthosis through a four-bar mechanism.

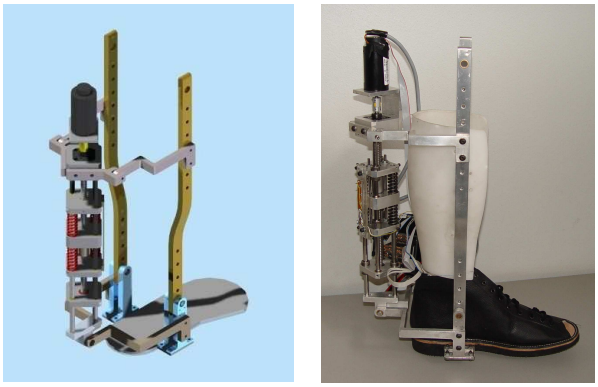

Figure 2. Active ankle-foot orthosis.

To reduce weight, most of the parts are made of duraluminum, a material with good mechanical strength and low density when compared with other aluminum alloys. Since it is under more stress than other parts, the orthosis foot was made of stainless steel. That material has greater mechanical strength but has also higher density, which increased the weight of the prototype. A polypropylene component was adapted and attached to the orthosis. This item gives the necessary support to accommodate the user leg in the orthosis. Diverse ways of connecting the exoskeleton to the user foot were studied, the chosen fixation method was the manufacturing of the orthopedic boot where the orthosis foot was used as structural component. The complete and test ready orthosis is shown in Figure 2.

3. Series Elastic Actuators

Traditional technologies for force control include current control with direct drive or geared actuator, force feedback through load cells, and fluid pressure control. In a direct drive actuator, a high quality servomotor is directly connected to the load and the torque output is accurately controlled using the relation between motor torque and motor current. However, servomotors operate inefficiently at the low speeds and high torques required in most robotic applications, which results in large and heavy units.

Alternatively, smaller and lighter servomotors can be used in low speed/high torque applications if a gear reduction is used. The reduction allows the motor to operate in high speed/low torque. However, the reduction gear has a few drawbacks such as friction and increasing the reflected inertia at the output of the gearbox. Since the factor of reduction

is very large, the impedance increases and control of force becomes inaccurate.

Even in the case of a geared actuator, you can minimize the friction and the effects of inertia by controller, measuring the force by a load cell. However, a load cell induces instabilities. In the case of a very fast linear motion, it can generate a pulse of very high strength. To maintain system stability is necessary small controller's gains. Therefore, the control is too slow, not responding to low-amplitude desired forces.

To overcome these shortcomings, the authors of (Pratt & Williamson 1995) proposed a force-controlled actuator, whose force sensor is a elastic element positioned in series with the load. This configuration is named Series Elastic Actuator.

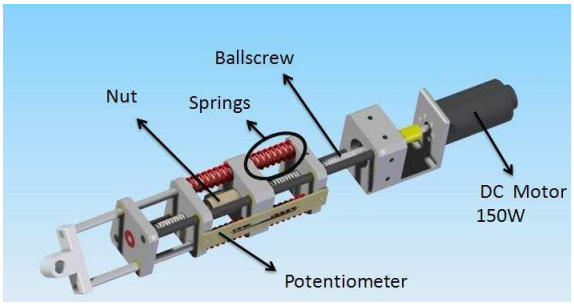

Figure 3. Series Elastic Actuator configuration.

The SEA presented in (Robinson et al. 1999), reproduced in the Figure 3, consists of a DC motor fixed to a ball screw through elastic coupling. The platform motion is driven by the nut, which converts the rotational ball screw movement into linear movement of the platform. To obtain force and impedance control of the actuator it is introduced a set of springs between the platform and the end effector. When the DC motor is driven, the nut moves forward or backward, compressing the pair of springs. The springs apply force to the load through the end effector.

The force and impedance control is done by measuring the spring deflection using a linear sliding potentiometer fixed in the two support platforms of the springs. Since the platforms are fixed in the two guides, the distance between them does not change. The potentiometer cursor is fixed in a nut support platform. When it moves, compressing the springs, the cursor moves up together, generating a voltage proportional to the springs deformation. By the Hooke's law, $F = -kx$, the force applied to the load is calculated.

The series elastic actuator shown in Figure 4, a similar reproduction of that presented in (Robinson et al. 1999), was constructed and assembled in our laboratory. To control the SEA, a power driver *EPOS* 70/10 (Maxon Motor), and a software developed in *Borland Builder C + +* is used.

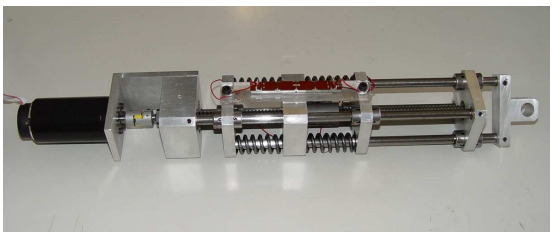

Figure 4. Series Elastic Actuator

3.1 Dynamic Model and Force Control

The SEA is modeled as a simple mass-spring-damper system, with equivalent motor mass m_m, damper coefficient b_m, and elastic constant k, given by:

$$m_m\ddot{x}_m + b_m\dot{x}_m = F_m - F_l, \tag{1}$$

with

$$F_l = k(x_m - x_l), \tag{2}$$

where x_m is the linear position of the lead-screw nut, x_l is the load position, F_m is the force generated by the motor and output force F_l. Actually, the damper coefficient b_m is found from the force and velocity constraint of the DC motor (Paluska & Herr 2006), that is,

$$b_m = \frac{F_{max}}{V_{max}}, \tag{3}$$

where F_{max} and V_{max} are maximum force and velocity the DC motor can reach, respectively. According to (Walsh et al. 2006), this estimate is considered a first approximation for the limitations of the DC motor and it is very similar to the limitations observed for a biological muscle.

Therefore, the force F_l, which drives the load, is function of F_m and x_l,

$$F_l(s) = \frac{F_m(s) - (m_m s^2 + b_m s)x_l(s)}{\frac{m_m}{k}s^2 + \frac{b_m}{k}s + 1}. \tag{4}$$

The force applied to the load is controlled by a closed loop system with feedback by measuring the deflection of the springs. A PD controller with a feedforward term provide the force control,

$$F_m = K_d\dot{e} + K_p e + F_d, \tag{5}$$

where $e = F_d - F_l$ is the error between the desired and measured forces, K_d and K_p are the PD gains and F_d and the desired force.

Combining equations (4) and (5) it is possible to determine the closed loop transfer function.

$$F_l(s) = \frac{(K_d s + K_p + 1)F_d(s) - (m_m s^2 + b_m s)x_l(s)}{\frac{m_m}{k}s^2 + \frac{b_m + kK_d}{k}s + (K_p + 1)}. \tag{6}$$

Figure 5 shows the block diagram of the proposed force control.

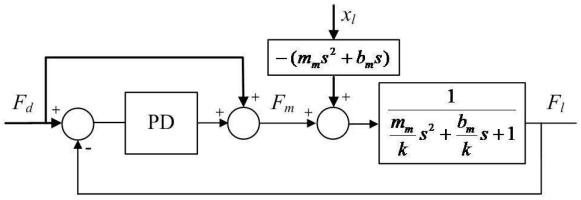

Figure 5. Closed Loop Force Control.

The results presented in Section 4consider the case where the load is fixed, that is, $x_l = 0$. Thus, closed loop transfer function is given by

$$\frac{F_l(s)}{F_d(s)} = \frac{K_d s + (K_p + 1)}{\frac{m_m}{k}s^2 + \frac{b_m + kK_d}{k}s + (K_p + 1)}. \tag{7}$$

This above equation shows how the applied force to the load behaves with the frequency of the desired input. For low frequencies, the function assumes 1, while at high frequencies,it tends to zero. Actually, it is shown in (Robinson et al. 1999) that the bandwidth of the SEA force control is reduced in comparison with a stiff actuator force control. However, the SEA improves the output power and the absorption of high frequency shocks (Paluska & Herr 2006).

3.2 Impedance Control

In this section the impedance control proposed in (Pratt, Willisson, Bolton & Hofman 2004) is adapted to be used in the variable impedance of the ankle-foot orthosis. The desired impedance is defined as the relationship between the load applied force F_l and the laod position x_l. It can be given as:

$$F_l = F_v - K_v x_l - B_v\dot{x}_l, \tag{8}$$

where F_v is a desired force to be applied to the load, K_v is the desired stiffness and B_v is the desired damping. The force F_v can be obtained by multipliyng the derised load position x_l^d by the desired sitffness K_v.

Using Eq. 2, the desired load position can be written as function of the desired motor position (actually, the variable to be commanded to to the inner loop position controller) and the load force:

$$x_l = x_m^d - \frac{F_l}{k}. \tag{9}$$

Substituting 9 in 8:

$$F_l = F_v - K_v x_m^d + \frac{K_v}{k} F_l - B_v \dot{x}_m^d + \frac{K_v}{k} \dot{F}_l. \tag{10}$$

The final term in the above equation contributes to noise due to the derivation of the force signal. Moreover, the value of k is in fact higher than the value of B_v. Therefore, this term can be leaved out in the control law. Since the motor is position-controlled through the position mode of the *EPOS* 70/10 driver, it is necessary to generate a solution to the desired motor position. Using the Euler approximation, a discrete control law can be generate from Eq. 10,

$$x_m^d(t) = \frac{F_v(t) + \frac{(K_v - k)}{k} F_l(t) + \frac{B_v}{\Delta t} x_m^d(t - \Delta t)}{K_v + \frac{B_v}{\Delta t}}. \tag{11}$$

for a given time t and a sampling period Δt. It is possible to notice that K_v e B_v should assume values higher than a certain minimum value to avoid excessive amplitudes for x_m^d.

4. Results

In this section we present the results obtained with the SEA shown in Fig. 4. Initially, force control is performed with the device not connected to the ankle-foot orthosis, with the end effector fixed (see Eq. 7). For the controller analysis was applied a desired step force of the $0N$ a $-100N$. The response to the step input is show in Figure 6.

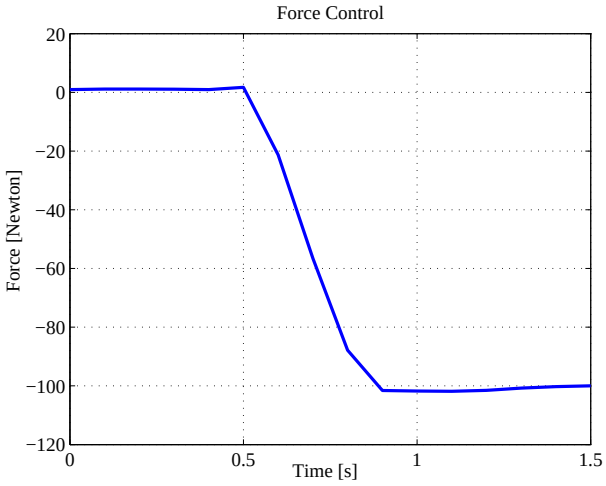

Figure 6. Step response 0N to -100N.

To test the ability of the SEA to simulate the behavior of a given impedance, the following set of experiments was considered: a spring-like behavior, a damper-like behavior and a spring-damper behavior. The values of K_v and B_v are introduced in the C++ program which computes the desired position for the motor and send it to the driver. The actual force value is computed considering the voltage measured through the potentiometer. For these experiments, the SEA was connected to the ankle-foot orthosis and an oscillatory force was applied in the ankle joint by the user, the results for the different behaviors of the device can be seen in Figures 7(a) to 7(c).

Figure 7(a) shows the actuator behaving like a spring of $K_v = 10N/mm$. Note that the displacement corresponds to the load force by a factor of 10. In Fig. 7(b), the actuator behaves like a damper with $B_v = 40\ Ns/mm$. In this case, the position follows the integral of the force, as expected. Figure 7(c) shows operation with both virtual damping ($B_v = 10\ Ns/mm$) and stiffness ($K_v = 10\ Ns/mm$). Note that, as expected, the spring-damper combination recovers with exponential decayment after load force is removed.

4.1 Variable Impedance Control Strategy

In this section, it is presented a control strategy to perform a variable impedance behavior in the active ankle-foot orthosis during the gait-pattern. To implement such a strategy, a state machine is considered with the following three states: controlled plantarflexion (CP), controlled dorsiflexion (CD) and swing phase. The first state starts at heel-strike and ends at foot-flat, describes the process by which the heel and forefoot initially makes contact with the ground. The ankle joint behaves like a linear spring, where joint torque is proportional to joint position. The controlled dorsiflexion begins at foot-flat and continues until when the foot takes off, storing the elastic energy necessary to propel the body.

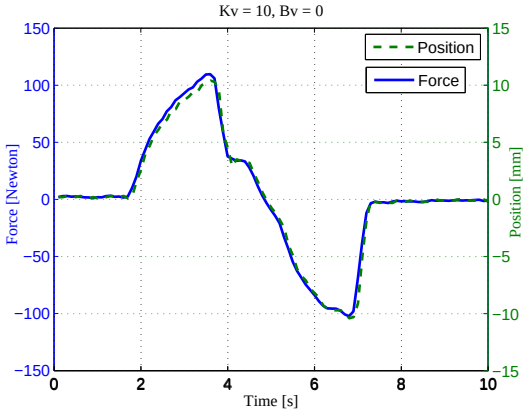

(a) Spring-like behavior.

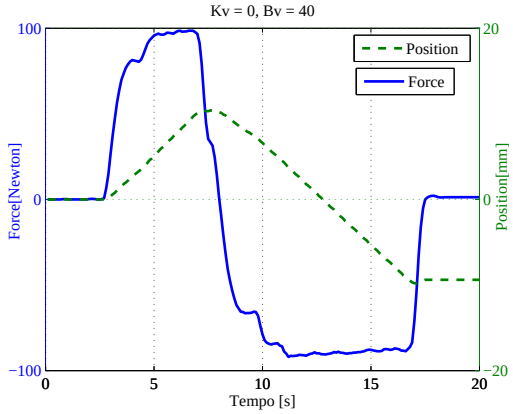

(b) Damper-like behavior.

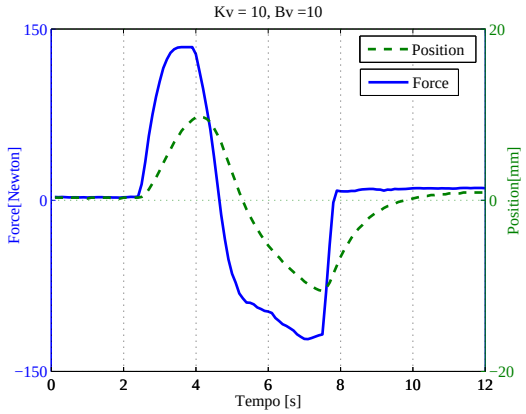

(c) Spring-damper behavior.

Figure 7. Series Elastic Actuator assuming differents impedances values.

Finally, the last state comprises the entire swing phase of the leg and ends when the heel contacts the ground, starting th next step.

During each state the actuator has a specific function behavior. According to (Au, Dilworth & Herr 2006), during the CP state, the ankle joint can be modeled as a linear torsional spring with elastic constant of $k_{CP} = 115$ Nm/rad; during the CD state, the ankle joint behaves again as a linear spring with $k_{DC} = 420$ N/rad; and finally, the swing phase may be represented by a second order mechanical model (spring-damper) with a spring constant $k_{SP} = 28,6$ Nm/rad and damper $B_{SP} = 0,57$ Nms/rad.

Therefore, the actuator's constants K_v and B_v must assume these values. Converting them to N/mm obtained:

Table 1. Impedance values of for each state.

State	k_v [N/mm]	B_v [Ns/mm]
Controlled plantarflexion	5,86	0,00
Controlled dorsiflexion	15,30	0,00
Swing phase	1,53	0,031

The variable impedance control strategy were implemented using 3 impedance states: K_1, K_2 and K_3 shown in table 1 and in Figure 8.

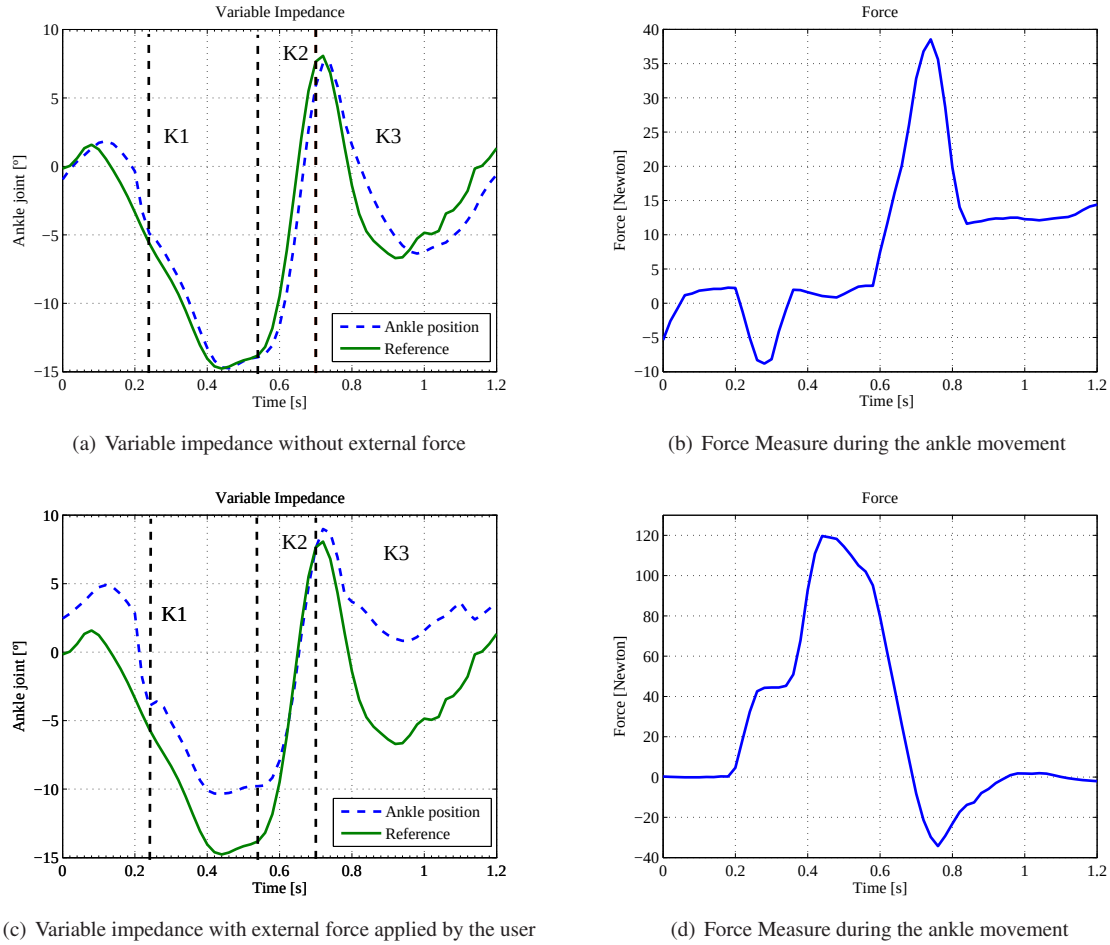

(a) Variable impedance without external force

(b) Force Measure during the ankle movement

(c) Variable impedance with external force applied by the user

(d) Force Measure during the ankle movement

Figure 8. Impedance analysis during the gait

The Figures 8(a) e 8(b) shown the orthosis behavior during the ankle joint movimentation where the user don't provide movement restriction. It is possible to note that the reference trajectory was followed by the orthosis in the 3 differents impedances and the force amplitude assumed low values. Figures 8(c) e 8(d) show the orthosis behavior when the user applies restricting force to the movement. The force magnitude assumes high values when the impedance is in the highest states, K_1 and K_2 and the reference trajectory were followed. In the low impedance state, K_3, the force magnitude decrease and the reference trajectory is not followed because in this case the user can moviment the orthosis easily.

To detect the states transition, FSR sensors were used and measures of position from the motor's encoder. The new sock containing contact sensors, FSR can be seen in Figure 9.

Figure 9. with FSR sensors.

As can be noted your shape fits better than the foot pad developed previously. The material is rubber which makes it flexible, comfortable and does not decreases the sensor sensitivity .

Through information from the encoder and using the relationships described in (12), obtain the foot position relative to the ground:

$$\theta_{ankle} = \arctan(\frac{P_{enc}}{4096b})\frac{180}{\pi}, \tag{12}$$

being P_{enc} encoder pulse number and b the length of the arm action.

The control was implemented in $C++$. When the heel is in contact with the ground the sensor 2 is activated (logic high level). The tibia has an angle less than zero on the position in which it is orthogonal to the foot (intermediate housing). Thus, the program enters the state of CP. When the angle of the tibia becomes positive and the sensor 2 is in contact with the ground, start up the DC state. At any time that the sensors are not being pressured (logical low level) the program enters the swing phase state.

Conclusions

This paper presented the results of implementing the force control in an series elastic actuator. It is noted that with the introduction of the series elastic it is possible to implement the force and impedance control and achieve performance similar to biological systems. The results show that the actuator is responding adequately to the data pulses. As future work seeks to implement the impedance control for the case free load and *zero* impedance, and the implementation of the device in the control of the active ankle-foot orthosis .

5. ACKNOWLEDGEMENTS

This work was supported by CNPq (Master scholarship) and FAPESP (Grant no. 2006/00006-5).

6. REFERENCES

Au, S. K., Dilworth, P. & Herr, H. (2006). An ankle-foot emulation system for the study of human walking biomechanics, *Proc. IEEE Int. Conf. on Robotics and Automation.*, Orlanda, Florida.

B., B. J. & Herr, H. (2004). Adaptative control of a variable-impedance ankle-foot orthosis to assist drop-foot gait, *IEEE Transactions on Neural Systems and Rehabilitation Engineering* **12**(1).

Chu, A., Kazerooni, H. & Zoss, A. (2005). On the biomimetic design of the Berkeley Lower Extremity Exoskeleton (BLEEX), *Proceedings of the the 2005 IEEE International Conference on Robotics and Automation*, Barcelona, pp. 4345 – 4352.

Kazerooni, H. (2005). Exoskeletons for human power augmentation, *Proceedings of the 2005 IEEE/RSJ International Conference on Intelligent Robots and Systems*, Edmonton,Canada.

Kim, S., Anwar, G. & Kazerooni, H. (2004). High-speed communication network for controls with the application on the exoskeleton, *Proceedings of the 2004 American Control Conference*, Boston, USA.

Paluska, D. & Herr, H. (2006). The effect of series elasticity on actuator power and work output: Implications for robotic and prosthetic joint design, *Robotics and Autonomous Systems* **54**: 667–673.

Pratt, G. A., Willisson, P., Bolton, C. & Hofman, A. (2004). Late motor processing in low-impedance robots: Impedance control of series-elastic actuators, *Proceedings of the 2004 American Control Conference*, Boston, Massachusetts, USA.

Pratt, G. & Williamson, M. (1995). Series elastic actuators, *Proceedings of the 1995 IEEE/RSJ International Conference on Intelligent Robots and Systems*, Vol. 1, Pittsburgh, pp. 399 – 406.

Pratt, J., Krupp, B. T. & Morse, C. J. (2004). The roboknee: An exoskeleton for enhancing strenght and endurance during walking, *Proceedings of the 2004 IEEE International Conference on Robotics and Automation*, New Orleans, LA.

Pratt, J. & Pratt, G. (1998). Exploiting natural dynamics in the control of a planar bipedal walking robot, *Proceedings of the Thirty-Sixth Annual Allerton Conference on Communication, Control, and Computing*, Urbana-Champaign, Illinois, pp. 561 – 568.

Robinson, D. W., Pratt, J., Paluska, D. & Pratt, G. (1999). Series elastic actuator development for a biomimetic walking robot, *Proceedings of the 1999 IEEE/ASME International Conference on Advanced Intelligent Mechatronics*, Atlanta, pp. 561 – 568.

Sensinger, J. W. & Weir, R. F. (2006). Improvements to series elastic actuators, *Mechatronic and Embedded Systems and Applications* pp. 1–7.

Walsh, C. J., Paluska, D. J., Pasch, K., Grand, W., Valiente, A. & Herr, H. (2006). Development of a lightweight, underactuated expskeleton for load-carrying augmentation, *Proceedings of the 2006 IEEE International Conference on Robotics and Automation*, Orlanda, Florida, pp. 3485–3491.

Zoss, A., Kazerooni, H. & Chu, A. (2005). On the mechanical design of the Berkeley Lower Extremity Exoskeleton (BLEEX), *Proceedings of the 2005 IEEE/RSJ International Conference on Intelligent Robots and Systems*, Edmonton, Canada, pp. 3465 – 3472.

7. Responsibility notice

The author(s) is (are) the only responsible for the printed material included in this paper